

# Size distributions of amylose and amylopectin solubilized from corn starch granules<sup>a</sup>

Size distributions of extracts derived from starch were investigated to aid in elucidating structure-function relationships of these polymers in water. Starch granules derived from waxy maize and amylo maize VII were dissolved in water by microwave heating in a high pressure vessel. Transmission electron microscopy of starch deposited from dilute solution and rotary shadowed with platinum, revealed that amylopectin imaged from waxy maize could be broadly classified as about 28% circular space filling patches containing branched clusters and 72% asymmetric linear containing branched clusters. Lengths of asymmetric linear amylopectin components ranged from about 37 to 980 nm whereas the diameter of circular amylopectin components ranged from about 44 to 200 nm. Although the starch in amylo maize VII is about 70% amylose, its narrow asymmetric structure when visualized by microscopy enabled us to image amylose even though amylopectin was present. Lengths of components ranged from about 46 to 254 nm. After smoothing and curve fitting, we found that all size distributions investigated could be treated as if they were multimodal in nature. The most abundant amylose component had a linear density of  $8.2 \times 10^3$  molar mass units/nm. This value could be explained if amylose had an aggregation number of about 5.9.

## INTRODUCTION

In many of its most important applications, starch must be dissolved or dispersed in aqueous media at a non-corrosive pH. Under these conditions, the constituent macromolecules of starch tend to aggregate, precipitate and/or gel (Young, 1984). Thus there have been comparatively few starch studies in neutral aqueous solution than in solvents in which starch is more soluble and stable (Roger & Colonna, 1992).

Since starch is a mixture of two chemically homogeneous polysaccharides, amylopectin and amylose, containing D-glucopyranosyl residues which differ with respect to glucopyranosyl linkage, hydrodynamic volume distribution, and molecular weight distribution, much effort has been expended in separating and characterizing them individually (Manners, 1989). These studies have revealed that amylopectin is among a group of macromolecules which consist of highly

branched structures containing a mixture of (1→4)- $\alpha$ -D-glucose and (1→6)- $\alpha$ -D-glucose linkages with molecular weights in the millions whereas amylose is much more linear with long stretches of (1→4)- $\alpha$ -D-glucose linked residues and molecular weights in the hundreds of thousands.

In this study, we visualized amylopectin solubilized from waxy maize. The starch in this variety of corn is practically pure amylopectin. Amylose was imaged from amylo maize VII. Because amylose is much more highly asymmetric under the microscope than amylopectin, we were able to visualize and quantitate the size distribution of amylose in the presence of amylopectin. Images were obtained by transmission electron microscopy on amylose and amylopectin rotary shadowed with platinum after being deposited onto mica from aqueous solution. Size distributions measured from these images were compared with size distributions measured earlier from high performance size exclusion chromatography (Fishman & Hoagland, 1994). In that study, scaling law constants obtained by plotting radius of gyration ( $R_g$ ) against molecular mass indicated that amylose and amylopectin were solubilized as dense fragments.

<sup>a</sup>Mention of brand names does not constitute an endorsement by the US Department of Agriculture over others of a similar nature not mentioned.

\*To whom correspondence should be addressed.

## MATERIALS AND METHODS

### Solubilization of starch

Waxy maize and amylo maize VII, commercial corn starches, were obtained from American Maize Products Co., Chicago, IL, USA. These starches had apparent amylose contents of 0% and 70%, respectively (Delgado *et al.*, 1991). Starches were solubilized by a procedure developed previously (Delgado *et al.*, 1991) with slight modifications. The procedure, detailed elsewhere (Fishman & Hoagland, 1994), consisted of placing a slurry of starch in water (4.4 mg/ml) into a microwave bomb, heating for 90 s in the microwave, cooling and centrifuging. Fishman and Hoagland (1994) found that about 49% of the starch derived from waxy maize and about 71% of the starch in amylo maize VII was solubilized.

### Transmission electron microscopy

Immediately after solubilized starch (waxy maize or amylo maize VII) solutions were cooled, they were diluted with HPLC grade water to 10 µg/ml. Aliquots (10 µl) were sandwiched between freshly cleaved pieces of mica (2 cm<sup>2</sup>) and allowed to set for 30 min. The sandwich was then peeled apart, mica was vacuum dried for 60 min at  $5 \times 10^{-6}$  torr, rotary shadowed with Pt at an angle of 5–8°, and coated with a layer of carbon. Coated replicas were floated off mica onto water, mounted on grids and examined by TEM in a Zeiss 10B electron microscope.

### Image analysis

Rotary shadowed images were recorded on photographic film at an instrumental magnification of 18,000×, as measured from the average spacings of a replica grating with 54,000 lines in. Visible particles of amylopectin or amylose were traced onto a transparent overlay with a marking pen. By this method, virtually all the visible particles on a photograph could be traced without duplication. The tracings were analyzed for contour length or circular diameter, digitized, and histograms (bin size 10 nm) were constructed from the digitized data using Imageplus software in a Dapple Systems (Sunnyvale, CA, USA) image analyzer.

### Curve fitting

Histograms of particle frequency plotted against contour length or diameter were converted to continuous distributions by smoothing, followed by curve fitting. The number of *i*th sized molecules ( $N_i$ ) in the histogram was smoothed to ( $N_{i,s}$ ) by adding one-half the incremental change to the lower bin value of adjacent values of ( $N_i$ ) as indicated by eqn (1) (Yau *et al.*, 1979).

$$N_{i,s} = N_i + \Delta N_i/2. \quad (1)$$

A continuous distribution was generated from the  $N_{i,s}$  values by fitting them to an envelope derived from a sum of overlapping Gaussian curves. The fit was obtained interactively with a non-linear regression program. The quarter band width or standard deviation ( $\sigma$ ) of all peaks was set equal. The value of ( $\sigma$ ) is a measure of the resolution of the component peaks in the smoothed distribution. Initial estimates of  $\sigma$  were obtained from the more completely resolved peaks at the upper end of the partially smoothed but not fitted size distribution. Initial estimates of peak heights, locations and number of peaks were by visual observation of the partially smoothed but not fitted distribution as well. All variables were adjusted with the aid of a curve fitting program ABACUS, which used a least-squares criterion for best fit (Draper & Smith, 1966). ABACUS was developed 'in house' and is coded in FORTRAN. Copies of the program can be obtained by writing to the authors.

## RESULTS AND DISCUSSION

### Size distributions of amylopectin

In Fig. 1A are transmission electron microscope (TEM) images of amylopectin solubilized from waxy maize starch granules by microwave heating and rotary shadowed with platinum at an angle of 5–8°. Yamaguchi *et al.* (1979) identified comparably shaped images from the TEM of negatively stained amylopectin extracted from waxy maize. For the purpose of imaging analysis, we have classified these images as either circular space filling patches containing branches or as asymmetric linear, containing branches and traced these images onto transparencies. Figure 2A contains tracings of the space filling patches whereas Fig. 2B contains tracings of the skeletal backbone of the asymmetric amylopectin. Based on 756 traced objects in photomicrographs containing both kinds of images, we found that 28.2% were space filling patches (SFP) and that 71.8% were asymmetric, linear (AL) structures.

A histogram was constructed from tracings of 1006 (SFP) shaped objects (Fig. 3a). A distribution was derived by smoothing and fitting the data. The smoothed data comprised six Gaussian shaped components (Fig. 4a). Because the objects in Fig. 2A are circular in shape, their diameters were obtained by measuring the area with an image analyzer and using computer software to calculate the diameter of a circle with equivalent area. Table 1 contains the diameter of each component at peak maximum, and these are numbered in the same order as they appear in Fig. 3a (left to right). Also included in Table 1 is the percentage of each component based on the area of the component

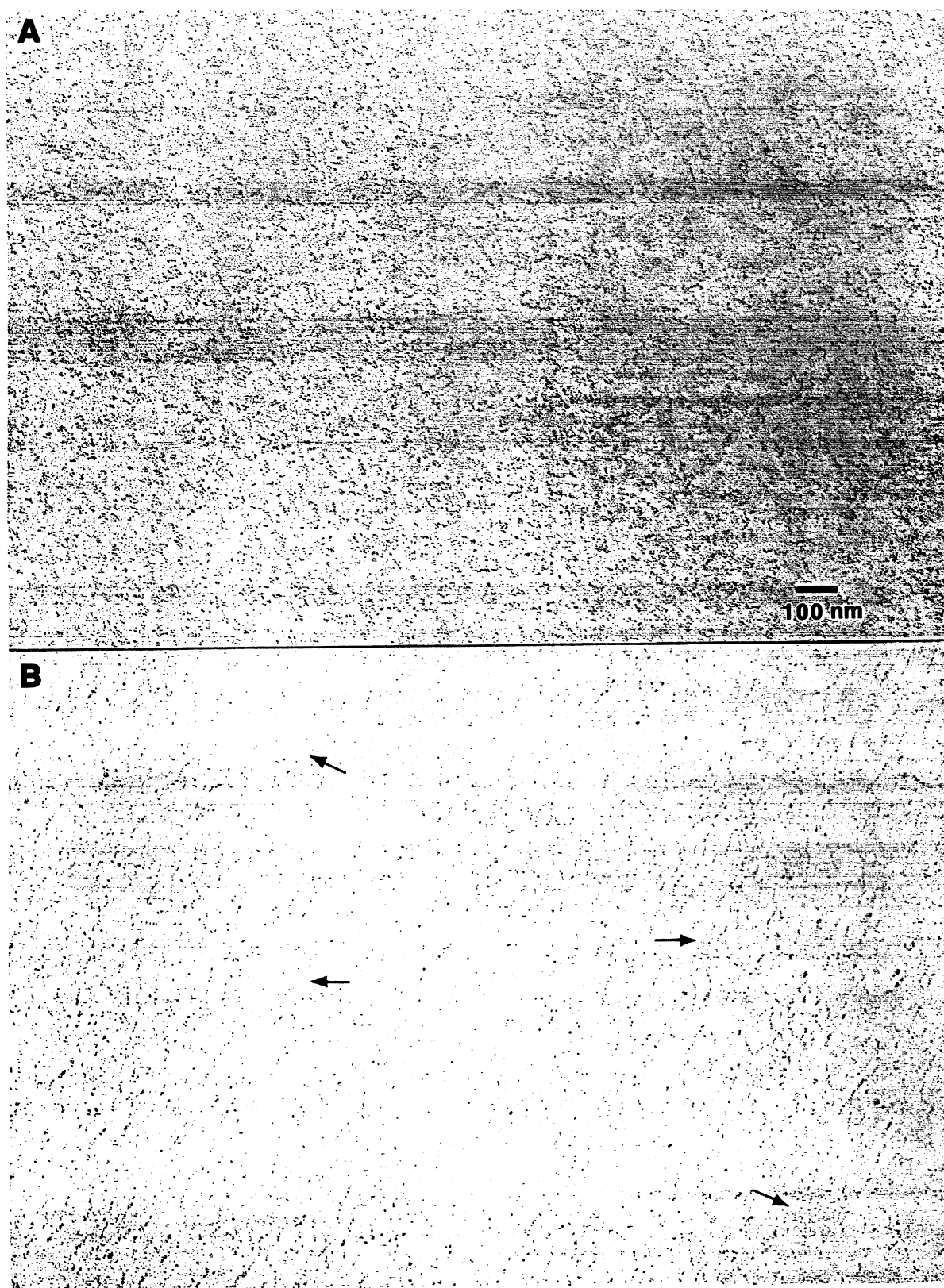


**Fig. 1.** (A) Rotary shadowed sample of amylopectin which was deposited onto freshly cleaved mica by the sandwich method at a concentration of  $10 \mu\text{g/ml}$ . Amylopectin forms two general shapes, circular space filling patches containing branched clusters and asymmetric linear containing branched clusters. Peak maxima of components from circular patches range in size from approximately 44 nm to about 200 nm. Component peak maxima of asymmetric linear shapes range in size from approximately 37 nm to about 980 nm. (B) Similar preparation of amylopectin VII revealed a few patches comparable to shapes identified as amylopectin (arrows) and numerous rod-like objects with component peak maxima ranging in length from 44.6–254 nm. Bar measures 100 nm.

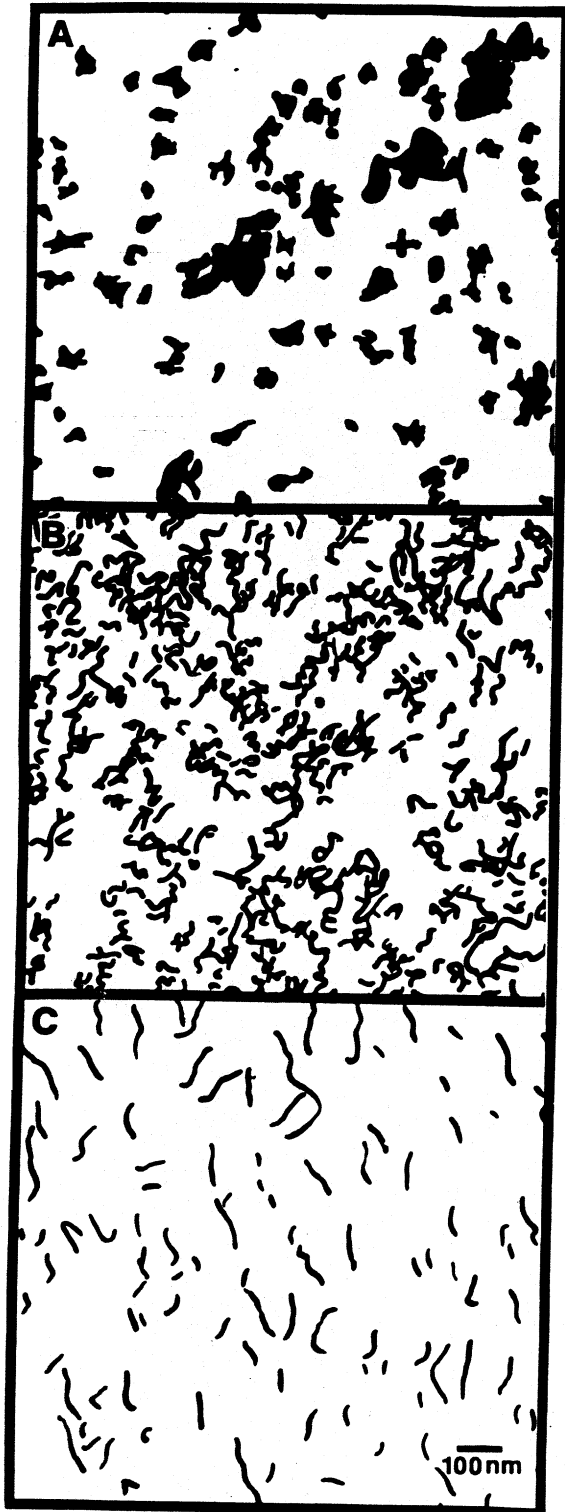
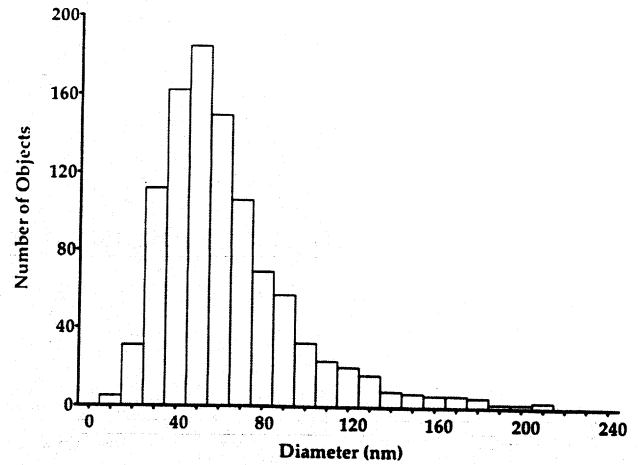
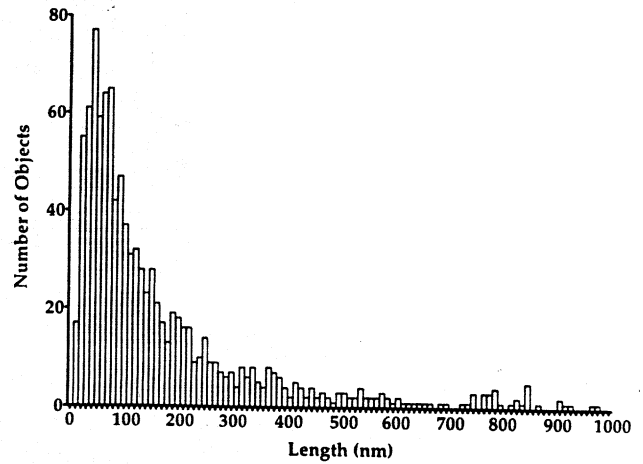


**Fig. 2.** Tracings of imaged starch. (A) Space filled patches of amylopectin. (B) Asymmetric linear shaped amylopectin. (C) Pseudo helical structure of amylose.

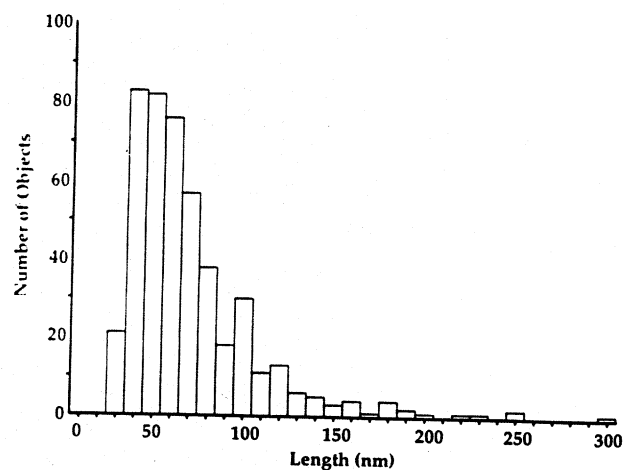
peak. By a similar process but utilizing linear skeletal backbone data such as in Fig. 2B, a histogram (Fig. 3b) and a smoothed distribution comprising 23 components (Fig. 4b) was constructed from 1010 (AL) objects.



(a)

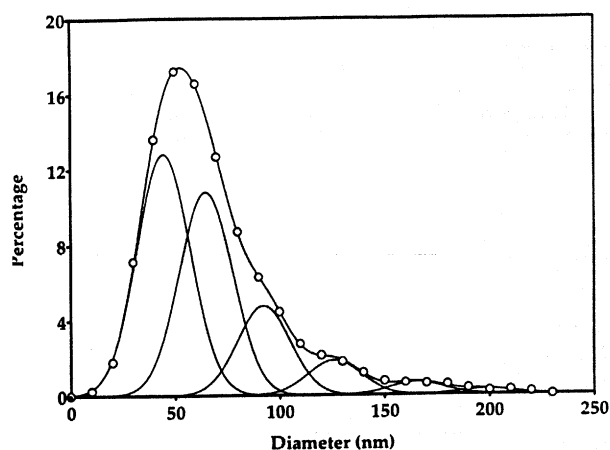


(b)

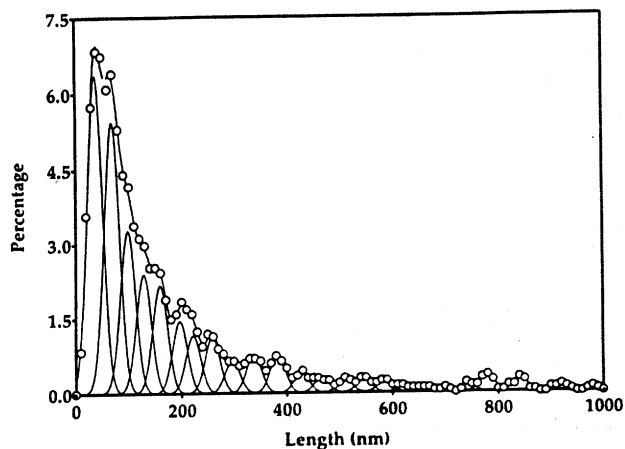


(c)

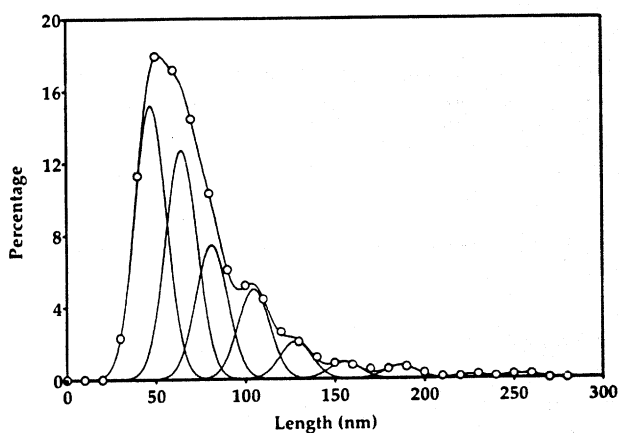
**Fig. 3.** Histogram of starch size distribution, bin size 10 nm. (a) Diameters of space filling patches (circular) of amylopectin, 1006 objects. (b) Lengths of asymmetric linear shaped amylopectin, 1010 objects. (c) Lengths of pseudo helical structure of amylose, 453 objects.



(a)



(b)



(c)

**Fig. 4.** Smoothed size distribution of starch. (a) Diameters of space filling patches of amylopectin comprising six components. Component peak resolution ( $\sigma$ ) 12.8 nm. (b) Lengths of asymmetric linear shaped amylopectin. Component peak resolution ( $\sigma$ ) 10.9 nm. (c) Lengths of pseudo helical structures of amylose. Component peak resolution ( $\sigma$ ) 8.93 nm.

**Table 1.** Diameters of space filling patch shaped amylopectin

Component <sup>a</sup>	Diameter (nm)	Percentage
1	44.6	41.1
2	64.9	34.6
3	92.4	15.2
4	126	6.0
5	166	2.2
6	200	0.9

<sup>a</sup>Component peak resolution,  $\sigma = 12.8$  nm.

**Table 2.** Contour lengths of asymmetric linear amylopectin

Component <sup>a</sup>	Length (nm)	Percentage
1	36.6	22.6
2	68.2	19.3
3	98.3	11.1
4	128	8.5
5	159	7.7
6	197	5.2
7	222	4.1
8	259	4.0
9	297	2.3
10	338	2.7
11	383	2.7
12	427	1.4
13	466	1.0
14	510	0.9
15	546	1.0
16	585	0.9
17	624	0.5
18	666	0.4
19	742	0.5
20	778	1.2
21	841	1.0
22	918	0.5
23	980	0.3

<sup>a</sup>Component peak resolution,  $\sigma = 12.9$  nm.

Table 2 contains the contour lengths at peak maximum of the skeletal backbone and percentages based on the area of each component peak in Fig. 4b. Table 3 contains the combined data for space filling patches and asymmetric, linear amylopectin. The percentage of each component has been recalculated taking into consideration that 28.2% of the material is SFP shaped amylopectin and that 71.8% is AL shaped amylopectin. Also included in Table 3 are the  $R_g$ s of the components at peak maximum and  $R_g$  values obtained from HPSEC for waxy maize starch prepared in a fashion similar to that used in this study (Fishman & Hoagland, 1994). The  $R_g$  values for the SFP amylopectin were calculated from the diameters by assuming that this form of amylopectin behaves as a hard sphere in solution according to eqn 2 (Marshall, 1978). AL amylopectin  $R_g$  values were calculated from the contour lengths by assuming wormlike chain behavior in solution according to eqn 3 (Chapman *et al.*, 1987).

$$R_g = (3/20)^{1/2} D \quad (2)$$

**Table 3. Sizes of asymmetric linear and space filling patches of amylopectin**

Microscope				HPSEC		
Component <sup>a</sup>	Length/Diam. <sup>b</sup> (nm)	Percentage	R <sub>g</sub> (nm)	Component <sup>b</sup>	R <sub>g</sub> (nm)	Percentage
				6	2.5	3
				5	5.2	5
				4	9.5	8
1	36.6	19.3	28.3			
1D	44.6	10.8	17.3			
2D	64.9	9.1	25.1			
2	68.2	16.1	26.6			
3D	92.4	4.0	35.8			
3	98.3	8.2	28.1			
4D	126	1.6	48.9			
4	128	5.3	31.1			
5	159	4.0	34.8			
5D	166	0.6	64.2			
6	197	3.4	39.4			
6D	200	0.2	77.6			
7	222	3.6	42.5			
8	259	2.7	46.9	2	44	24
9	297	2.2	51.1			
10	338	1.2	55.4			
11	383	1.4	59.9			
12	427	1.4	64.1			
13	466	0.7	67.4			
14	510	0.5	71.2			
15	546	0.5	74.2			
16	585	0.5	77.3			
17	624	0.5	80.2			
18	666	0.2	83.3			
19	742	0.6	88.5			
20	778	0.5	91.0			
21	841	0.6	95.0	1	95	46
22	918	0.3	99.8			
23	980	0.2	103			

<sup>a</sup>Component peak resolution,  $\sigma = 8.93$  nm.

<sup>b</sup>To conform with notation in Fishman and Hoagland (1994) the components identified in HPSEC chromatograms are numbered largest size 1, smallest size 6. In HPSEC, the largest component elutes first whereas the smallest elutes last. The order of components from imaging of micrographs as numbered by the software is smallest size 1, largest size 23. Components of comparable size from the two techniques are on the same line in the table.

$$R_g^2 = a_0^2 \{L/3a_0^2 - 1 + 2a_0/L[1 - \exp(-L/a_0)]\}. \quad (3)$$

In eqn 2,  $D$  is the diameter of the SFP amylopectin. In eqn 3,  $a_0$  is the persistence length which we take as 36.6 nm, the contour length of the smallest AL component observed in the microscope and  $L$  is the contour length.

Comparison of length and diameter global averages (Table 4) reveals that SPF diameters tend to be smaller than AL lengths for comparable averages. Thus when the two shapes are combined, comparable global average lengths fall between the two shapes.

Comparison of  $R_g$ s of components from microscope images with those from HPSEC (Table 3) reveals microscope  $R_g$ s ranging from 17 to 103 nm whereas those obtained from HPSEC ranged from approximately 3 to 95 nm. Approximately 85% of the radii measured by HPSEC fall in the same range as found by microscopic measurement. Comparison of component distributions obtained from the two methods reveals

**Table 4. Global averages of amylopectin lengths/diameters (nm)**

Type	Number	Weight	Z
SPF	67.8	80.9	98.8
AL	170	357	550
Comb.	134	311	531

that the preponderance of  $R_g$ s measured by the microscope were below 43 nm whereas most of the components measured by HPSEC were above 43 nm. Comparison of global averages (Table 5) reveals that weight and z-averages of radii are larger from measurement by HPSEC than by microscope as expected from comparison of component distributions. The number average radius for HPSEC was lower than that measured by microscope because components 4, 5, and 6 from HPSEC which have  $R_g$ s below 17 nm are not observed by microscopy. This result probably occurs

**Table 5. Global averages of amylopectin radii of gyration (nm)**

Type	Number	Weight	Z
SPF	26.2	31.3	38.3
AL	36.2	57.3	74.5
Comb.	37.6	48.0	64.0
HPSEC <sup>a</sup>	20	60	81

<sup>a</sup>Taken from Fishman and Hoagland (1994).

because of the inherent ability of HPSEC columns to discriminate between components in a lower size range than the microscope whereas the microscope has the ability to discriminate in higher size ranges than HPSEC columns. Given the higher size range capabilities of the microscope over those of HPSEC columns, the question arises as to why the weight and z-averages measured by HPSEC were about 25% higher than the comparable averages measured by microscopy (see Table 5). As mentioned in the Introduction, starch in neutral aqueous solution is subject to aggregation and ultimately precipitation. In the HPSEC study, as in the present study, we attempted to measure the starch samples as rapidly as possible after microwave solubilization to minimize aggregation. Preparation of the sample for HPSEC required a membrane filtration step not required for microscopic analysis of the sample. Possibly, during the time required to filter the starch for analysis by HPSEC (~15 min), the HPSEC samples became more aggregated than the samples imaged by microscopy. We note also that only six components were required to describe the distribution obtained from HPSEC whereas 23 components were required to describe the distribution obtained by microscopy. The difference in the number of components indicates a significantly higher component peak resolution for the microscope than for HPSEC.

### Size distributions of amylose

In Figure 1B rotary shadowed images of starch are solubilized from amylo maize VII. This sample was solubilized and prepared for microscopy in a fashion similar to the preparation used for amylopectin.

As was the case with amylopectin, objects in Fig. 1B were traced onto transparencies (Fig. 2C). Histograms were constructed by measuring the contour lengths of the linear skeleton of the tracings (Fig. 3c). From the data obtained in this manner, a smoothed, fitted distribution comprising 13 Gaussian shaped components was derived (Fig. 4c). Whereas objects from several microscopic fields were combined to obtain amylopectin distributions, objects in four separate fields were averaged in the case of amylose. Microscopic data were based on the 2755 objects imaged. Average lengths and percentages for amylose components are given in Table 6. Standard deviations are in parentheses. Also included

in the table are values of  $R_g$  calculated by assuming that amylose is rod-like in shape according to eqn 4 (Marshall, 1978)) and values of  $R_g$  obtained from HPSEC (data taken from Fishman & Hoagland, 1994).

$$R_g = L/(12)^{1/2} \quad (4)$$

where  $L$  is the length of the rod.

Amylo maize VII, the source of amylose, has been reported to have an apparent amylose:amylopectin ratio of 70:30 (Delgado *et al.*, 1991). Comparison of the TEM photomicrograph of amylose (Fig. 1B) with that from waxy maize (Fig. 1A) revealed that the amylo maize VII photomicrograph contained only a few images similar to the space filling patches found in the photomicrograph obtained from waxy maize even though approximately 30% of amylo maize VII was amylopectin. Comparison of images from waxy maize (Fig. 1A) with those from amylo maize VII (Fig. 1B) reveals that the contrast is much higher in the amylo maize micrographs. The images from amylo maize VII were very similar to the pseudo helical structure reported in the literature for amylose synthesised enzymatically and lightly substituted with carboxymethyl groups (Stokke & Elgsaeter, 1991). Thus, it is possible that the amylopectin present in amylo maize is not as visible as amylose due to differences between the two in platinum shadowing. As in the case of synthetic amylose, our micrographs indicated that the amylose molecules derived from amylo maize, were uniformly oriented. The features in common between the amylose studied in this work and the synthetic amylose studied by Stokke and Elgsaeter occurred in spite of several differences in sample preparation. In this work starch was deposited from distilled water, samples were rotary shadowed, and deposited on mica by the sandwich method. Synthetic amylose was deposited from buffered 50% glycerol, directionally shadowed and deposited by the mica by spraying from a nebulizer. Comparisons revealed some differences apparent in preparations from the two studies as well. The proximity of molecules and some evidence of clustering indicated the presence of a loose gel structure in our preparation as contrasted with the distinctly individual molecules found in preparations of synthetic amylose. Possibly these differences arise from the absence of glycerol in our preparation. Previously, in the case of pectin, TEM showed that glycerol dissociated hydrogen bonded pectin gels into their component parts (Fishman *et al.*, 1993). Nevertheless, it was shown in that study that the length distribution of the component gel parts could be obtained even when glycerol was absent from the polysaccharide solvent. Furthermore, starch gels are much looser than pectin gels so that the individual components are readily recognisable. Unlike synthetic amylose which had a monodisperse length distribution, amylose derived from amylo maize had a broad distribution (Figs 3c, 4c).

In Table 6, we have calculated  $R_g$ s from microscope

Table 6. Sizes of amylose

Microscope				HPSEC		
Component <sup>a</sup>	Length	%	$R_g$ (nm)	Component <sup>b</sup>	$R_g$ (nm)	%
				6	3.0 (0.1)	7 (1)
				5	4.9 (0.2)	16 (1)
				4	8.0 (0.4)	25 (2)
				3	14 (1)	27 (1)
1	46.1 (1.1)	38 (3)	13.3			
2	64.1 (0.6)	29 (2)	18.5			
3	82.2 (1.7)	15 (2)	23.7			
4	103 (2)	8.8 (1.6)	29.9	2	29 (2)	13 (1)
5	125 (3)	4.6 (0.5)	36.2			
6	150 (4)	2.4 (0.2)	43.3			
7	173 (1)	2.3 (0.3)	49.9			
8	187 (1)	1.3 (0.4)	54.0			
9	201	0.5	58.0			
10	219	0.9	63.3			
11	228 (2)	0.4 (0.1)	65.9			
12	242	0.6	69.9			
13	254	0.5	73.4	1	73 (5)	11 (1)

<sup>a</sup>Component resolution,  $\sigma = 8.53$  (0.9).

<sup>b</sup>To conform with notation in Fishman and Hoagland (1994) the components identified in HPSEC chromatograms are numbered largest size 1, smallest size 6. In HPSEC the largest component elutes first whereas the smallest elutes last. The order of components from imaging of micrographs as numbered by the software is smallest size 1, largest size 13. Components of comparable size from the two techniques are on the same line in the table. Standard deviations are shown in parentheses.

derived contour lengths by assuming a rod-like model and comparing these with  $R_g$ s obtained from HPSEC measurements. Microscope values of  $R_g$  ranged from about 13 to 73 nm whereas values from HPSEC ranged from 3 to 73 nm. For both methods of obtaining  $R_g$ , the most abundant sized molecule had an  $R_g$  of 13 or 14 nm (i.e. component 1 by microscope or component 3 by HPSEC). Analysis by HPSEC-Viscometry revealed that components 1 and 2 from that technique are probably a mixture of amylose and amylopectin whereas components 3–6 probably contain all amylose (Fishman & Hoagland, 1994). For amylose, as was the case for amylopectin, microscopy appeared to resolve the components better than HPSEC in the range of size overlap (13–73 nm) for the two techniques. In that range, microscopy gave 13 components whereas there were only six components from HPSEC.

Table 7 contains the global size averages for amylose. The number average  $R_g$  from HPSEC is lower than the microscope value due to HPSEC components 4–6 which were not found in the micrographs. The  $\bar{z}$ -average radius from HPSEC was found to be higher than the microscope value due to a greater percentage of objects with radii above 29 nm found by HPSEC than by microscope. Possibly this finding was due to the presence of amylopectin in components 1 and 2. Stokke and Elgsaeter found that the synthetic amylose had a length of 270 nm and a molecular weight per unit length ( $M_L$ ) of 1440 molar mass units/nm. As can be seen from Tables 6 and 7 the amylose molecules visualized in this study were much smaller in length. The most abundant component from microscopy and HPSEC which also

Table 7. Global averages of amylose sizes (nm)

	Number	Weight	Z
Length			
Microscope	72 (3)	85 (3)	109 (7)
$R_g$			
Microscope	21 (1)	25 (1)	31 (2)
HPSEC <sup>a</sup>	10 (1)	20 (2)	41 (4)

<sup>a</sup>Taken from Fishman and Hoagland (1994). Standard deviations are shown in parentheses.

had the same  $R_g$  (Table 6), had an  $M_L$  value of about  $8.2 \times 10^3$  molar mass units/nm based on a molar mass of about 380,000 (Fishman & Hoagland, 1994), possibly indicating that this amylose had an aggregation number of 8.2/1.4, or about 5.9. That result is consistent with chain thicknesses observed in Fig. 1B. On the assumption of rod-like behavior, components 4, 5 and 6 from HPSEC have  $M_L$  values of 4.0, 2.1,  $1.1 \times 10^3$ , respectively. The aggregation numbers for these components would be about 2.9, 1.5 and 0.79, respectively. Chain length dependent aggregation could explain low values in solution for scaling law constants when plotting  $R_g$  or intrinsic viscosity against molar mass for amylose in solution (Roger & Colonna, 1993; Fishman & Hoagland, 1994).

## CONCLUSIONS

We have shown that there are two broad shape classes present in amylopectin extracted by the microwave

method used in this report. The asymmetric linear structure with branches predominates, encompasses a wider size range than circular amylopectin, and is much larger. The skeletal backbone of AL amylopectin is better approximated by the worm-like chain whereas amylose is best approximated by the rod-like chain. We concluded this by comparing  $R_g$ s obtained from microscope measurements with those obtained from HPSEC. Finally, it is possible to readily characterize distributions of amylose by microscopy in the presence of amylopectin, thus avoiding time-consuming physical separations.

#### ACKNOWLEDGEMENT

We thank Kahlila S. Johnson for her able technical assistance with electron microscopy and size analysis of amylose.

#### REFERENCES

- Chapman, H.D., Morris, V.J., Selvandran, R.R. & O'Neill, M.A. (1987). Static and dynamic light scattering studies of pectic polysaccharides from the middle lamellae and primary cell walls of cider apples. *Carbohydr. Res.*, **165**, 53-68.
- Delgado, G.A., Gottfried, D.J. & Ammeraal, R.N. (1991). Maize starch sample preparation for aqueous size exclusion chromatography using microwave energy. In *Biotechnology of Amylodextrin Oligosaccharides*, ed. R.B. Friedman. ACS Symposium Series 458, Washington DC, p. 405.
- Draper, N. & Smith, H. (1966). In *Applied Regression Analysis*. John Wiley, New York, pp. 267-70.
- Fishman, M.L., Cooke, P., Hotchkiss, A. & Damert, W. (1993). Progressive dissociation of pectin. *Carbohydr. Res.*, **248**, 303-16.
- Fishman, M.L. & Hoagland, P.D. (1994). Characterization of starches dissolved in water by microwave heating in a high pressure vessel. *Carbohydr. Polym.*, **23**, 175-83.
- Manners, D. (1989). Recent developments in our understanding of amylopectin structure. *Carbohydr. Polym.*, **11**, 87-112.
- Marshall, A.G. (1978). In *Biophysical Chemistry, Principles, Techniques & Applications*. John Wiley, New York, p. 477.
- Roger, P. & Colonna, P. (1992). The influence of chain length on the hydrodynamic behavior of amylose. *Carbohydr. Res.*, **227**, 73-83.
- Roger, P. & Colonna, P. (1993). Evidence of the presence of large aggregates contaminating amylose solutions. *Carbohydr. Polym.*, **21**, 83-9.
- Stokke, B.T. & Elgsaeter, A. (1991). Electron microscopy of carbohydrate polymers. In *Advances in Carbohydrate Analysis*. JAI Press, Vol. 1, pp. 195-247.
- Yamaguchi, M., Kainuma, K. & French, D. (1979). Electron microscopic observations of waxy maize starch. *J. Ultrastruct. Res.*, **69**, 249-61.
- Yau, W.W., Kirkland, J.J. & Bly, D.D. (1979). In *Modern Size-Exclusion Chromatography*. John Wiley, New York, pp. 318.
- Young, A.H. (1984). Fractionation of starch. In *Starch, Chemistry & Technology*, eds R.L. Whistler, J.N. BeMiller & E.F. Paschall. Academic Press, Orlando, Florida, pp. 249-83.